**Astronomy
&
Astrophysics**

Formation of simple organic molecules in inner T Tauri disks

M. Agúndez[1], J. Cernicharo[1], and J. R. Goicoechea[2]

[1] Departamento de Astrofísica Molecular e Infrarroja, Instituto de Estructura de la Materia, CSIC, Serrano 121, 28006 Madrid, Spain
e-mail: [marce;cerni]@damir.iem.csic.es

[2] LERMA-LRA, UMR 8112, CNRS, Observatoire de Paris and École Normale Supérieure, 24 rue Lhomond, 75231 Paris Cedex 05, France
e-mail: javier@lra.ens.fr

ABSTRACT

Aims. We present time dependent chemical models for a dense and warm O-rich gas exposed to a strong, far ultraviolet (FUV) field aimed at exploring the formation of simple organic molecules in the inner regions of protoplanetary disks around T Tauri stars.
Methods. An up-to-date chemical network is used to compute the evolution of molecular abundances. Reactions of H_2 with small organic radicals such as C_2 and C_2H, which are not included in current astrochemical databases, overcome their moderate activation energies at warm temperatures and become very important for the gas phase synthesis of C-bearing molecules.
Results. The photodissociation of CO and release of C triggers the formation of simple organic species such as C_2H_2, HCN, and CH_4. In timescales between 1 and 10^4 years, depending on the density and FUV field, a steady state is reached in the model in which molecules are continuously photodissociated, but also formed, mainly through gas phase chemical reactions involving H_2.
Conclusions. The application of the model to the upper layers of inner protoplanetary disks predicts large gas phase abundances of C_2H_2 and HCN. The implied vertical column densities are as large as several 10^{16} cm^{-2} in the very inner disk (<1 AU), in good agreement with the recent infrared observations of warm C_2H_2 and HCN in the inner regions of IRS 46 and GV Tau disks. We also compare our results with previous chemical models studying the photoprocessing in the outer disk regions, and find that the gas phase chemical composition in the upper layers of the inner terrestrial zone (a few AU) is predicted to be substantially different from that in the upper layers of the outer disk (>50 AU).

Key words. astrochemistry – stars: circumstellar matter – stars: planetary systems: protoplanetary disks – ISM: molecules – ISM: planetary nebulae: general

1. Introduction

Protoplanetary disks (PPDs) represent an intermediate stage in the evolution from dark clouds toward planetary systems. A detailed characterization of the physical and chemical conditions in such disks is of great interest, as they provide the initial conditions for planet formation (see Najita et al. 2007; Bergin et al. 2007 for recent reviews on the subject). Information about the disk chemical composition has mainly come from radio observations, which are sensitive to the outer cool disk, from ~100 AU up to ~900 AU (Dutrey et al. 1997; Thi et al. 2004). Only recently, the inner regions of PPDs have been probed by means of infrared observations revealing the presence of warm C_2H_2 and HCN with large gas phase abundances (Lahuis et al. 2006; Gibb et al. 2007) and of complex organic species such as polycyclic aromatic hydrocarbons (PAHs) (Geers et al. 2006; Habart et al. 2006).

Chemical models have mostly concentrated in the study of the outer disk regions (e.g., Aikawa & Herbst 1999), in part motivated by radio observations of several molecular species. Only a few models have focused on the inner disk (<10 AU) chemistry. Willacy et al. (1998) studied the chemistry in the disk midplane, shielded from stellar and interstellar UV photons, and found that some organic species could be easily formed on grain surfaces. Markwick et al. (2002) studied the chemistry in the inner 10 AU, including stellar and interstellar UV radiation, stellar X-rays, and radionuclides decay as sources of ionization and adsorption/desorption on grains, but not mantle chemistry,

i.e., formation and destruction of molecules occurs only in the gas phase. They calculated large abundances of organic species such as CH_4 but they did not discuss the main chemical routes to form them. Semenov et al. (2004) and Ilgner & Nelson (2006) extensively discussed the ionization degree over a wide range of radii and heights over the midplane. Woods & Willacy (2007) predicted that benzene formation can be efficient in the midplane of the inner disk (<3 AU), a dense region protected against UV photons where grain surface reactions play an important role in building up a complex organic chemistry.

In this paper, we investigate gas phase routes to form simple organic molecules, such as acetylene (C_2H_2), hydrogen cyanide (HCN), and methane (CH_4) in a dense and warm oxygen-rich gas exposed to a strong FUV field ($h\nu < 13.6$ eV). We apply this model to the inner region (<10 AU) of a protoplanetary disk around a T Tauri star and compare with the abundances recently derived from observations.

2. Chemical model

Physical models of protoplanetary disks suggest a flared-up structure where both the gas density and temperature vary enormously, depending on the radius r from the star and height z over the disk equatorial plane (see Dullemond et al. 2007 for a review). The gas density decreases radially outward as a power law of r, and in the vertical direction it decreases as z increases in roughly an exponential way. The gas heating across the disk

is dominated by the stellar irradiation of the surface layers at large radii ($r \geq 10$ AU), thus, the kinetic temperature increases with z, while at small radii ($r \sim$ a few AU) viscous dissipation may become an important heating mechanism in the midplane regions (D'Alessio et al. 1998, 1999). A flared disk is significantly exposed to the strong UV field from the central star. The extinction of stellar UV radiation is large in the midplane, but it rapidly decreases as z increases. Therefore, there exists a layer of low A_V where the disk material is being photoprocessed (Aikawa & Herbst 1999; Willacy et al. 2000). Here we focus on the chemistry that takes place in the photon-dominated region (PDR) of the inner disk ($r < 10$ AU), where typically temperatures are several hundreds of degrees Kelvin, and gas densities range from 10^6 to 10^{11} cm^{-3}.

In order to qualitatively understand the chemical routes to form simple organic molecules in the PDR of the inner disk, we have first performed a few time dependent chemical models in which chemical abundances evolve under fixed physical conditions representative of this region. We consider an O-rich gas with all the hydrogen initially as H_2, all the carbon as CO, the oxygen in excess as H_2O, and all the nitrogen as N_2. We use solar abundances (Asplund et al. 2005) and assume that 50% of C and 65% of O are in carbon and silicate grains respectively. Therefore, the initial abundances relative to the total number of H nuclei n_H, where $n_H = 2\,n(H_2) + n(H)$, are $x(CO) = 1.25 \times 10^{-4}$; $x(H_2O) = 3.5 \times 10^{-5}$; $x(N_2) = 3.0 \times 10^{-5}$; and $x(He) = 8.5 \times 10^{-2}$. We adopt a gas density of $n_H = 2 \times 10^8$ cm^{-3} and run several models with five different kinetic temperatures: $T_k = 100$, 300, 500, 750, and 1000 K.

We first consider a *FUV illuminated* model with a FUV field strength of $\chi = 50\,000$ (relative to the Draine interstellar radiation field; Draine 1978), the value at 10 AU according to FUV observations of various T Tauri disks (Bergin et al. 2003, 2004). For this FUV field and gas density, photoprocessing of the gas occurs in a range of visual extinctions $A_V \sim 0.1$–5. If $A_V \lesssim 0.1$, the gas is very exposed to the UV radiation and molecules are destroyed, and in the case of $A_V \gtrsim 5$ photoprocessing occurs only marginally. Here, we investigate the chemical evolution at a mean extinction value of $A_V = 2.5$. We then consider a separate *X-ray illuminated* model in which the gas is solely exposed to X-rays, but not FUV photons, aiming at evaluating the influence of these two energy sources on the chemistry. There is evidence for X-ray emission in protoplanetary disks (Feigelson & Montmerle 1999). The main effect of X-rays on the chemistry is the ionization of the gas producing high-energy photoelectrons (ph-e$^-$), which further ionize and dissociate the species. To simulate this effect we have enhanced the cosmic ray ionization rate by a factor of 1000 over the standard interstellar value, we thus assume $\zeta = 1.2 \times 10^{-14}$ s^{-1}, which is reasonable for the inner regions of PPDs (Igea & Glassgold 1999).

We use the chemical code described in Cernicharo (2004). The species included in the model are given in Table 1. We selected them on the basis of previous calculations, including a larger number of species that allowed us to identify the most important chemical processes forming C-bearing species. The chemical network used was taken from Cernicharo (2004) and Agúndez & Cernicharo (2006), and was checked against the NIST chemical kinetics database[1] and the latest version of the UMIST database for astrochemistry[2] (Woodall et al. 2007). We include neutral-neutral and ion-molecule bimolecular reactions, three body processes and thermal dissociations.

[1] See http://kinetics.nist.gov/kinetics/index.jsp
[2] See http://www.udfa.net

Table 1. Species included in the model.

H	C_2H	NH_2	C+	CH_5+	HCO+	CN+
H_2	C_2H_2	NH_3	C-	C_2+	HOC+	CN-
He	O_2	CN	O+	C_2H+	H_2CO+	HCN+
C	OH	HCN	O-	C_2H_2+	H_3CO+	HCNH+
O	H_2O	HNC	N+	C_2H_3+	CO_2+	N_2H+
N	CO	H_2CN	H_2+	OH+	HCO_2+	H_2NC+
CH	CO_2	NO	H_3+	OH-	N_2+	CNC+
CH_2	HCO	e-	CH+	H_2O+	NH+	NO+
CH_3	H_2CO	H+	CH_2+	H_3O+	NH_2+	HNO+
CH_4	N_2	H-	CH_3+	O_2+	NH_3+	HNC+
C_2	NH	He+	CH_4+	CO+	NH_4+	

Important reactions involved in the build up of small organic molecules at high temperatures are those of H_2 with radicals such as C_2 and C_2H. These reactions have been studied in the laboratory over a relatively wide temperature range: $C_2 + H_2 \rightarrow C_2H + H$ between 295 and 493 K (Pitts et al. 1982) and $C_2H + H_2 \rightarrow C_2H_2 + H$ in the range 178–440 K (Peeters et al. 1996; Opansky & Leone 1996). They have moderate activation barriers of about 1400 K, which make them very slow in the cold interstellar medium, although at high temperatures they become rapid enough to control the abundance of C-bearing species. Their rate constant expressions are not included in current astrochemical databases, which are somewhat biased toward low temperature chemistry, but can be found in Table 1 of Cernicharo (2004). The formation of H_2 on grain surfaces is included with a rate constant of 3×10^{-17} cm^3 s^{-1}.

In order to properly take into account FUV line self-shielding, we explicitly calculated a grid of H_2 and CO photodissociation rates and C photoionization rates, appropriate for the physical conditions in the inner disk. We performed this calculation with the *Meudon PDR code* (Le Bourlot et al. 1993). The model has been described in detail elsewhere (Le Petit et al. 2006; Goicoechea & Le Bourlot 2007). In particular, we computed the depth dependent FUV radiation field for the range of parameters (χ, n_H, T_k and initial abundances) considered in the *FUV illuminated* model. The H_2, CO, and C photorates were then consistently integrated over these fields and used afterwards in the time-dependent chemical calculations. Dust properties are known to influence the resulting rates (e.g., Goicoechea & Le Bourlot 2007). Here, we have assumed the standard grain size distribution proposed for the interstellar medium (ISM) (Mathis et al. 1977). We took all the other photorates included in the *FUV illuminated* model from the UMIST 2006 database. In the *X-ray illuminated* model we have included reactions induced by X-rays for which we have adopted the cosmic ray induced reactions rates enhanced by a factor of 1000.

3. Chemical routes to C_2H_2, HCN and CH_4

The left panels in Fig. 1 show the evolution of C_2H_2, HCN, and CH_4 abundances for several gas temperatures in the *FUV* model. The synthesis of these organic species can be divided into three steps.

(i) Photodissociation of CO and N_2 with release of atomic C, C$^+$ (produced by further photoionization of C) and atomic N. The timescale of this step depends only on the FUV field strength, thus on χ and A_V.

(ii) Atom → molecule transition, from the primary species C, C$^+$, and N to simple C-containing molecules. Important
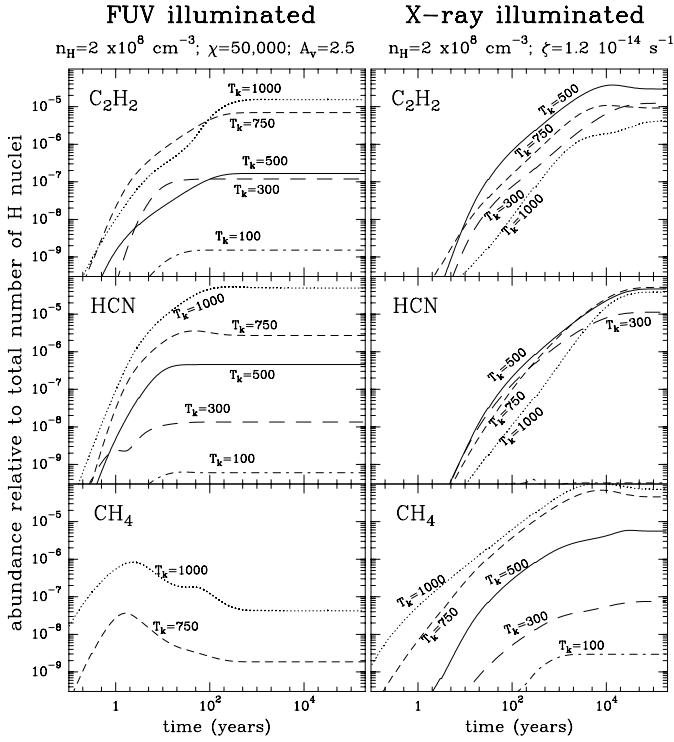
Fig. 1. Evolution of C_2H_2, HCN, and CH_4 abundances for a chemistry driven by FUV photons (*left*) and by X-rays (*right*). Different curves correspond to different gas temperatures.

reactions that drive this transition are (see Fig. 2) radiative associations such as $C + H_2 \rightarrow CH_2 + h\nu$ and $C^+ + H_2 \rightarrow CH_2^+ + h\nu$, and rapid neutral-neutral reactions such as $C + NO \rightarrow CN + O$, where NO comes from the reaction between N and OH. These reactions are nearly temperature independent, thus their rate depends basically on the gas density: the higher the gas density the faster they proceed. Bimolecular reactions such as $C^+ + H_2 \rightarrow CH^+ + H$ and $C + H_2 \rightarrow CH + H$ begin to overcome their activation barriers at temperatures above 400 and 700 K, respectively. Three body reactions are not competitive, compared to radiative associations, for gas densities below $\sim 10^{13}$ cm^{-3}.

(iii) Processing of simple molecules, CH_2, CH_2^+, and CN, into more complex species, represented by C_2H_2, HCN, and CH_4 in our model. As Fig. 2 shows, this processing occurs through bimolecular reactions involving H_2, C, and N. Reactions of neutral species with H_2 have energy barriers higher than 1000 K, which introduces a strong temperature dependence. This is very marked for CH_4 because its formation involves the reactions with the highest energy barriers, making it abundant only at temperatures above ~ 700 K. The synthesis of organic molecules in the O-rich gas requires that atomic carbon, produced by the dissociation of CO, incorporates into C-bearing species faster than reverting to CO. This is achieved by different mechanisms at low and high temperatures. At temperatures below ~ 400 K atomic oxygen is not converted into OH (the reaction $O + H_2 \rightarrow OH + H$ has an activation energy of ~ 5000 K) and the main CO-forming reaction, $OH + C \rightarrow CO + H$, is inhibited. Thus atomic carbon can react with other species instead of reverting to CO. The main obstacle to form C-bearing species at low temperature is the energy barrier of several reactions. For example, C_2H_2 and HCN reach low abundances at 100 K because the reactions

of C_2H and CN with H_2 have activation barriers. At temperatures above ~ 400 K atomic oxygen is efficiently converted into OH, which may react with C to form CO but reacts faster with H_2 to form water. Thus, most of the oxygen forms H_2O, and CO does not reach its maximum abundance allowing atomic carbon to form C-bearing molecules. At high temperatures most of the reactions shown in Fig. 2 overcome their energy barriers producing a rich C-based chemistry.

The chemistry driven by X-rays (see right panels in Fig. 1) is similar to that initiated by FUV photons except that the dissociation of CO and N_2, step i, is carried out by collisions with photoelectrons: $CO + ph\text{-}e^- \rightarrow C + O$ and $N_2 + ph\text{-}e^- \rightarrow N + N$ and by reactions with He$^+$: $CO + He^+ \rightarrow C^+ + O + He$ and $N_2 + He^+ \rightarrow N + N^+ + He$. For our chosen FUV and X-ray field strengths, these reactions are about 100 times slower than photodissociations, which increases the chemical timescale by roughly the same factor, i.e., molecules form later (see Fig. 1). On the other hand, the lower dissociating strength of X-rays, compared to that of the FUV field, results in a higher steady state abundance of C-bearing molecules. This occurs because these steady state abundances depend on the balance between the rates at which molecules are formed (through chemical reactions) and are destroyed (by either FUV photons or X-rays). The destruction rates are lower in the *X-ray* model compared to the *FUV* model and, thus, chemical reactions have more time to form molecules until steady state is reached. As a consequence, in the *X-ray* model C_2H_2 and HCN reach high abundances with little dependence on the temperature, once this is above a threshold value of about 300 K (necessary for some important reactions to overcome their energy barriers). Thus, the main differences in the *FUV* and *X-ray* models arise because of the different dissociating strengths. In fact, if the ionization rate is enhanced by a factor of 100 in the *X-ray* model, then the evolution of the molecular abundances, and their steady state values, become much closer to those of the *FUV* model.

The relative intensity between the FUV and X-ray fields will establish whether the chemistry is dominated by FUV photons (PDR) or X-rays (XDR). X-rays will drive the chemistry in those regions of protoplanetary disks with a column density toward the star $\gtrsim 10^{22}$ cm^{-2}; these regions are shielded against FUV photons ($A_v > 5$), but not against X-rays (Maloney et al. 1996). In regions with column density values of $\gtrsim 10^{25}$ cm^{-2}, X-rays are severely attenuated and do not affect to the chemistry.

In summary, according to the models, the formation of acetylene, hydrogen cyanide, and methane occurs in timescales between a few years and a few thousands of years, and is clearly favored at high temperatures. They reach a steady state in which they are destroyed by photodissociation (or X-ray induced reactions) and reactions with H, but are continuously reformed through reactions involving H_2. Thus, the relative rates between reformation and destruction will determine the steady state abundance. A high abundance of H_2, maintained due to its continuous formation on grain surfaces, is essential for accelerating the process

$$A + H_2 \rightarrow AH + H \qquad (1)$$

where A is an atom or simple radical. In this way, organic species AH can reach a high steady state abundance. In fact, if the formation of molecular hydrogen on grain surfaces is suppressed, then H_2 is effectively dissociated (due to its continuous participation in reactions of the above type) in about 10^3–10^4 years in the *FUV* model and 10^6 years in the *X-ray*
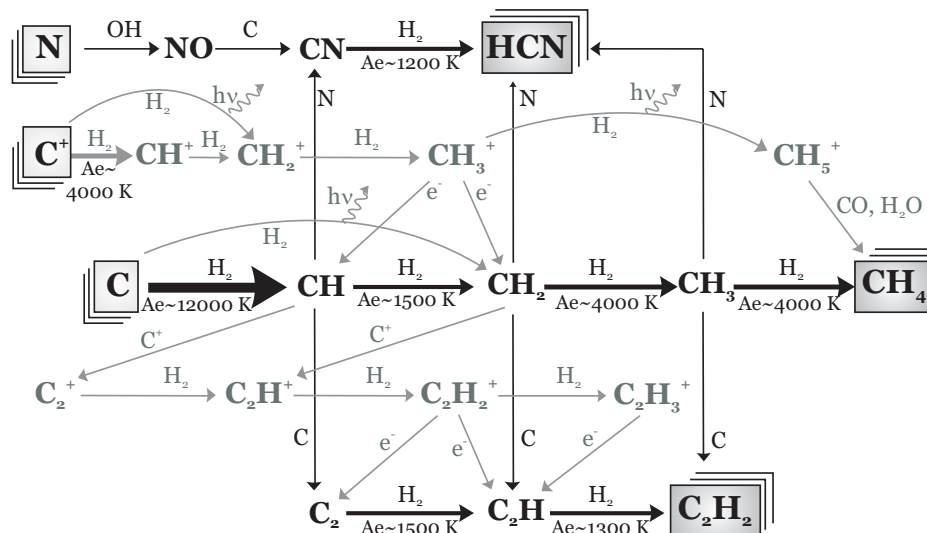
Fig. 2. Scheme with the main synthetic routes for the formation of C_2H_2, HCN, and CH_4 from C, C^+, and N. Reactions with a high activation energy (Ae) are indicated by a thick arrow.

model, a time at which most of the molecules are also destroyed, thus becoming transient species.

The steady state abundances of C_2H_2, HCN, and CH_4 are very sensitive to the kinetic temperature (especially in the *FUV* model), and may vary from $<10^{-10}$ at 100 K up to several 10^{-5} at 1000 K. The chemistry of these simple organic molecules also depends, although to a lesser extent, on other parameters of the model. The FUV/X-ray field and gas density affect the chemical timescale (a decrease in any of these parameters will make the chemistry proceed slower) as well as the steady state abundance (higher n_H/χ or n_H/ζ ratios favor the formation of molecules compared to the destruction by FUV photons or X-rays and thus favor a higher steady state abundance). The C/O ratio is also an important parameter that affects the wealth of C-bearing molecules. Obviously, values close to 1 favor a rich C-based chemistry, while low values make it more difficult. We, nevertheless, find that only when adopting C/O ratios substantially lower than the solar value (0.54; Asplund et al. 2005) do the abundances of C-bearing species decrease appreciably. The choice of the initial abundances is also an issue when modeling the chemistry in protoplanetary disks and several options have been used in the literature (see, e.g., Willacy et al. 1998; Semenov et al. 2004). If we assume an initial atomic composition, instead of a molecular one, we find that the chemical timescale is noticeably reduced (the step i has been already carried out) although the steady state abundance is essentially the same. The non-dependence of steady state abundances on the initial composition is a consequence of the strong photoprocessing of the material, and indicates that molecular abundances in the PDR of inner disks are not affected by the chemical history of the gas. The actual situation in PPDs may be different if mixing motions bring material from outer cold regions and affect the chemical balance in the PDR.

At this point it would be interesting to discuss our results by comparing them with some other PDR models that have appeared in the literature. A detailed study of the chemistry in PDRs has been carried out by Sternberg & Dalgarno (1995). They modeled a dense ($n_H = 10^6$ cm^{-3}) and highly irradiated ($\chi = 2 \times 10^5$) plane parallel cloud. They considered a reduced set of chemical species, including S- and Si-bearing molecules, of low-chemical complexity (e.g., they did not included species with more than one carbon atom). The calculated steady state abundances for C-bearing molecules such as HCN and CH_4 are lower than 10^{-9} in the warm region of $A_V = 0$–2 ($T_k = 3000$–50 K), although radicals such as CH have abundances as high as 10^{-6}. The most remarkable difference between their model and ours lies in the n_H/χ ratio. The much smaller value of this ratio used in their model (5 compared to our adopted value of 4000) favors photoprocesses compared to chemical reactions and results in low abundances of closed-shell organic molecules. A more recent PDR model by Teyssier et al. (2004) and Pety et al. (2005), focuses on the study of long carbon chains in PDRs such as the Horsehead Nebula. They consider a model with a gas density of $n_H = 2 \times 10^4$ cm^{-3} and a FUV field strength of $\chi = 60$, thus the n_H/χ ratio is 300, which is much closer to the value we adopted. Their model, nevertheless, predicts C-chains, such as C_2H and C_4H, to have abundances of $\leq 10^{-8}$. The different results reached by their model and ours could be due to a different chemical network used, but are most likely related to the different values of the kinetic temperature. In their model, the abundance of hydrocarbon radicals peaks in the region of $A_V = 1$–2, where T_k is lower than 100 K. At these relatively low temperatures, hydrocarbons do not reach high abundances since their formation is inhibited by various reactions, which have moderate activation barriers.

4. Abundances in the inner region of a T Tauri disk

The physical conditions adopted in the chemical models discussed in the previous section are assumed to be representative of those prevailing in the PDR of inner T Tauri disks. Nevertheless, real conditions at different points (r, z) in such disks span over a wide range around our adopted values. In order to check whether photochemistry can account for the formation of simple organic molecules with abundances comparable to those observed, we have adopted the disk physical structure, gas density and temperature at each point, from a steady state flared accretion disk model provided by P. D'Alessio (D'Alessio et al. 1998, 1999). The disk model has a mass accretion rate $\dot{M} = 10^{-8}$ $M_\odot$ yr^{-1}, grain properties similar to those of interstellar dust (maximum dust grain size is 0.25 μm), and a central star with $M_* = 0.7$ $M_\odot$, $T_* = 4000$ K and $R_* = 2.6$ $R_\odot$. The chemical model was run for a grid of 18×16 ($r \times z$) points covering
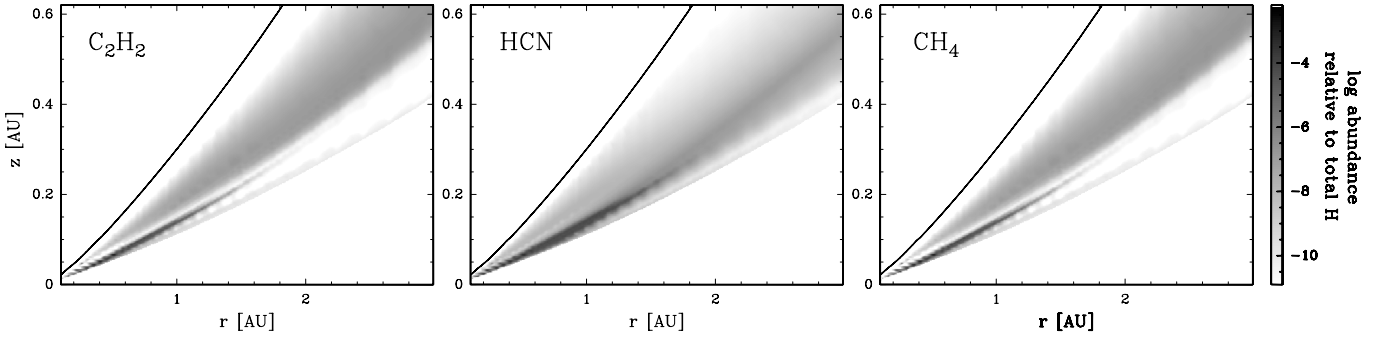
Fig. 3. Distribution of C$_2$H$_2$, HCN, and CH$_4$ abundances in the photodissociation region of the inner 3 AU of a protoplanetary disk. The solid line indicates the disk surface, as given by the height z_∞ (see D'Alessio et al. 1999).

the upper layers of the very inner disk $r = 0.1$–3 AU. The modeled region covers the CO/C/C$^+$ transition, from an inner height z_{in} (where the gas is well shielded against stellar and interstellar light and all the carbon is as CO) up to the disk surface defined by the height z_∞ (where the gas is completely exposed to the FUV field and all the carbon is as C$^+$, see Fig. 3).

We consider that gas is affected by stellar and interstellar FUV radiation and by cosmic rays. For simplicity, we neglect the effect of stellar X-rays, although in the case of strong X-ray emitter T Tauri stars the abundances of certain molecules, which are sensitive to the ionization rate such as HCO$^+$ or HNC, may be substantially affected. The influence of an enhanced ionization rate on the molecular abundances has been discussed by Aikawa & Herbst (1999) and Markwick et al. (2002). Concerning the formation of simple organics such as C$_2$H$_2$, HCN, and CH$_4$, an enhanced ionization rate does not greatly change the results from those obtained when only a FUV radiation field is considered.

We treat the FUV field considering that each point (r, z) of the disk is exposed to two separate radiation fields, stellar and interstellar. The FUV flux emanating from the star is diluted geometrically and attenuated by the column density of material in the line of sight toward the point (r, z). Interstellar radiation is assumed to penetrate into the disk in the vertical direction. For simplicity, the radiative transfer of stellar and interstellar FUV photons is treated separately, in a plane parallel $1 + 1$D approach. The computed depth-dependent H$_2$, CO, and C photorates are then used in the grid of time-dependent chemical models. Although a coupling between the attenuation of the FUV field and the molecular abundances exists, a self-consistent 2D solution of the radiative transfer problem, together with the chemical evolution, is beyond the scope of this study.

The spectral shape of the FUV field emitted by a T Tauri star significantly differs from that of the interstellar radiation field (ISRF). Therefore, photodissociation/ionization rates can be drastically different in the presence of a T Tauri radiation field compared to an enhanced ISRF. This problem has been addressed by van Dishoeck et al. (2006), who calculated photodissociation/ionization rates of various species for a 4000 K blackbody radiation field, typical of T Tauri stars, and compared with the values obtained under the ISRF. They found that, for the same integrated flux between 912 and 2050 Å, the photorates of species such as H$_2$, CO, or N$_2$ decrease by several orders of magnitude when the stellar radiation field, instead of the ISRF, is used.

Given the impact of the true stellar radiation field on the photochemistry, we have used the *Meudon PDR code* to generate a new grid of depth-dependent H$_2$ and CO photodissociation rates and of C photoionization rates. Instead of

adopting a given ISRF enhancement, the FUV field is generated by a T Tauri star simulated by a blackbody at 4000 K and a stellar radius of 2.6 $R_\odot$. The intensity in the Lyα line, at 1216 Å, can be very important in T Tauri stars (Bergin et al. 2003), and can have a large impact on the photorates of some species, such as OH and CH$_4$, although it does not affect the photorates of other species such as H$_2$, CO, and N$_2$ because their main photoabsorption bands lie short of 1216 Å. For simplicity, here, we do not consider enhanced emission at the Lyα line. The resulting radiation field at the disk surface is then determined by the geometrical dilution from the star. We obtain stellar photorates for H$_2$, CO and C that are about 5 orders of magnitude smaller than the ISRF photorates (for the same integrated flux in the FUV), in agreement with the values reported by van Dishoeck et al. (2006). Stellar photorates for species other than H$_2$, CO, and C are taken from van Dishoeck et al. (2006) when available, or are otherwise assumed to be equal to the ISRF photorates. The visual extinction of stellar and interstellar light at a given point is assumed to be proportional to the column density of hydrogen nuclei N_H in the direction toward the star and outward in the vertical direction, respectively. We use the standard relation $A_V = N_H$ (cm^{-2}) / 1.87×10^{21} (Bohlin et al. 1978), adequate for the ISM grain size distribution. In the modeled region, the stellar FUV field has a strength that is higher than the ISRF by orders of magnitude ($\chi = 10^4$–10^7). However, since the stellar photorates are for many species lower than the ISRF photorates by orders of magnitude, the photoprocessing of the material in the PDR layers is to a great extent dominated by the interstellar, rather than stellar, FUV radiation field.

The gas densities are 10^8–10^{11} cm^{-3} in the sampled region and the gas kinetic temperature, assumed equal to the dust temperature in the disk physical model, ranges from 100 to 1000 K. According to Kamp & Dullemond (2004), the gas temperature significantly exceeds the dust temperature in the very upper layers with a visual extinction of stellar radiation $A_V < 0.1$. In this superheated surface layer our model most probably underestimates the gas temperature. The implications, however, for the calculated abundances of simple organic species are small since this is a region where CO has fully dissociated and most of the carbon is as C$^+$. We do not consider adsorption/desorption on dust grains since at the high temperatures prevailing in the studied layers ($T_k > 100$ K) all the molecules should have been evaporated from grain mantles and should be in the gas phase.

The abundance distributions at time 10^4 yr, when steady state has been reached, for C$_2$H$_2$, HCN, and CH$_4$ are plotted in Fig. 3. A thin shell of the disk contains simple organic species with abundances ranging from 10^{-8} (in the outer part, at 2–3 AU)
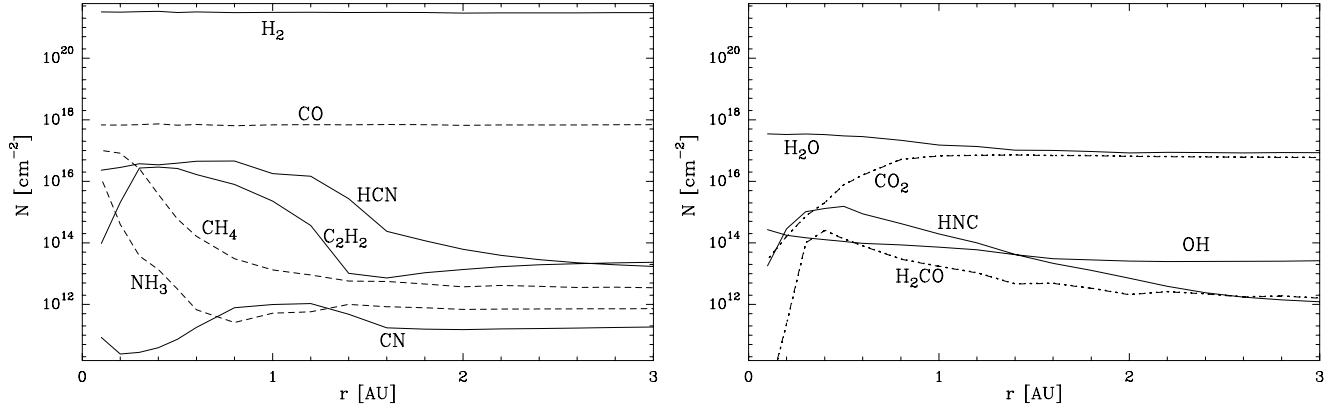
Fig. 4. Vertical column densities within the PDR of the inner 3 AU of a protoplanetary disk. They are computed by integrating the gas molecular densities from the inner height z_{in} to the disk surface z_∞.

up to 10^{-4} (in the inner 1 AU where gas is hot). The amount of material contained in such a thin layer is, however, remarkably large due to the large gas densities prevailing there. Vertical column densities within the disk PDR can be calculated by integrating the gas molecular densities in the z direction (see Fig. 4). The column densities of H_2 and CO are also shown to visualize the molecular abundances relative to these two species.

Lahuis et al. (2006) observed toward IRS 46 hot (>350 K) C_2H_2, HCN, and CO_2 with column densities of 3, 5, and 10×10^{16} cm^{-2}, respectively. In GV Tau, Gibb et al. (2007) detected warm C_2H_2 and HCN with column densities of 7 and 4×10^{16} cm^{-2}, respectively, and derived an upper limit for methane of CH_4/CO < 0.0037, rather similar to that found by Gibb et al. (2004) in HL Tauri (CH_4/CO < 0.005). The inferred warm temperatures led these authors to suggest that both acetylene and hydrogen cyanide are most likely located in the inner disk, within a few AU around the star. In our model, the vertical column densities of C_2H_2 and HCN are a few 10^{16} cm^{-2} in the inner 1 AU, but noticeably decrease as r increases following the decrease in temperature. The column densities of these two species could be enhanced at radii larger than 1 AU if the gas temperatures are higher than in our disk model or if vertical and radial mixing brings warm material toward the cooler midplane regions, as has been suggested for CO in the outer regions of PPDs (Semenov et al. 2006). Our model predicts that CH_4 has a large abundance in the very inner disk (<0.5 AU). However, it is less abundant than C_2H_2 and HCN throughout the rest of the disk, unlike in the model by Markwick et al. (2002) where it is the most abundant organic species. The reasons for this difference are unclear. In the model by Markwick et al. (2002), the large gas phase abundance of methane is likely due to its desorption from grain surfaces. However, since they do not include formation of molecules on grain surfaces, CH_4 must have been previously formed through a mechanism of gas phase reactions, which is not explicitly detailed. We, nevertheless, do not model the same disk region studied by Markwick et al. (2002). We only consider the upper disk layers exposed to FUV radiation, while they consider the full disk in the z direction down to the midplane, where most of material is contained. Thus, the vertical column densities of H_2 in our modeled region are $\sim 10^{21}$ cm^{-2}, while in their model the column densities are $\sim 10^{25}$ cm^{-2}, so that the large abundances of CH_4 they calculate are coming from a region much closer to the midplane than in our model. This makes a direct comparison between both models difficult.

In our model, CO_2 is formed very efficiently through the reaction between CO and OH, and has a fairly large column density of about 10^{17} cm^{-2}, which agrees with the value observed toward IRS 46 by Lahuis et al. (2006). Figure 4 also gives the column densities of some other molecules which, although have not been observed in the inner regions of T Tauri disks, are predicted to have relatively large column densities in the PDR. The molecule H_2CO is formed with a moderate abundance through various reactions involving atomic oxygen and small hydrocarbon radicals. The presence of HNC is strongly related to that of HCN, since it is formed through proton transfer to the latter species and subsequent dissociative recombination. The column density of NH_3 has a radial profile similar to that of CH_4, but with a value about one order of magnitude lower. Also, it is interesting to note that the abundance ratio of a closed-shell molecule and its related radical (e.g., H_2O/OH and HCN/CN) is quite large (about 100–1000), in contrast with the values close to 1 predicted in the outer disk, $r > 50$ AU, (e.g., Willacy et al. 2000). This is a consequence of the large gas densities prevailing in the inner disk which, in spite of the strong FUV field, tend to favor the formation of closed-shell species through reaction (1).

5. Conclusions

In summary, we have shown that a strong FUV/X-ray field may efficiently drive a rich C-based chemistry in a dense O-rich gas with kinetic temperatures of several hundreds of degrees Kelvin. The application of our PDR chemical model to the inner regions of a T Tauri disk yields gas phase abundances for simple organic molecules, such as C_2H_2 and HCN, that range from 5×10^{-5} to 10^{-8}, depending on the radius. This translates into vertical column densities as large as 10^{17} cm^{-2} in the very inner disk (<1 AU) down to 10^{13} at 3 AU. The model thus explains the large column densities of C_2H_2 and HCN (several 10^{16} cm^{-2}) observed in the inner regions (a few AU) of IRS 46 and GV Tau disks (Lahuis et al. 2006; Gibb et al. 2007). The huge variations with radius of the gas density and temperature within the PDR layer of protoplanetary disks results in a quite different gas phase chemistry, i.e., different molecular abundances and ratios between them, in the inner terrestrial zone compared to the outer regions at several hundreds of AU. Our results await confirmation from further observations of different molecular species probing the inner regions of protoplanetary disks.

References

Agúndez, M., & Cernicharo, J. 2006, ApJ, 650, 374

Aikawa, Y., & Herbst, E. 1999, A&A, 351, 233

Asplund, M., Grevesse, N., & Sauval, A. J. 2005, in Cosmic Abundances as Records of Stellar Evolution and Nucleosynthesis, ed. T. G. Barnes III, & F. N. Bash (San Francisco: ASP), ASP Conf. Ser., 336, 25

Bergin, E., Calvet, N., D'Alessio, P., & Herczeg, G. J. 2003, ApJ, 591, L159

Bergin, E., Calvet, N., Sitko, M. L., et al. 2004, ApJ, 614, L133

Bergin, E. A., Aikawa, Y., Blake, G. A., & van Dishoeck, E. F. 2007, in Protostars and Planets V, ed. B. Reipurth, D. Jewitt, & K. Keil (Tucson: Univ. Arizona Press), 751

Bohlin, R. C., Savage, B. D., & Drake, J. F. 1978, ApJ, 224, 132

Cernicharo, J. 2004, ApJ, 608, L41

D'Alessio, P., Cantó, J., Calvet, N., & Lizano, S. 1998, ApJ, 500, 411

D'Alessio, P., Calvet, N., Hartmann, L., et al. 1999, ApJ, 527, 893

Draine, B. T. 1978, ApJS, 36, 595

Dullemond, C. P., Hollenbach, D., Kamp, I., & D'Alessio, P. 2007, in Protostars and Planets V, ed. B. Reipurth, D. Jewitt, & K. Keil (Tucson: Univ. Arizona Press), 555

Dutrey, A., Guilloteau, S., & Guélin, M. 1997, A&A, 317, L55

Feigelson, E. D., & Montmerle, T. 1999, ARA&A, 37, 363

Geers, V. C., Augereau, J.-C., Pontoppidan, K. M., et al. 2006, A&A, 459, 545

Gibb, E. L., Rettig, T., Brittain, S., et al. 2004, ApJ, 610, L113

Gibb, E. L., Van Brunt, K. A., Brittain, S. D., & Rettig, T. W. 2007, ApJ, 660, 1572

Goicoechea, J. R., & Le Bourlot, J. 2007, A&A, 467, 1

Habart, E., Natta, A., Testi, L., & Carbillet, M. 2006, A&A, 449, 1067

Ilgner, M., & Nelson, R. P. 2006, A&A, 445, 205

Igea, J., & Glassgold, A. E. 1999, ApJ, 518, 848

Kamp, I., & Dullemond, C. P. 2004, ApJ, 615, 991

Lahuis, F., van Dishoeck, E. F., Boogert, A. C. A., et al. 2006, ApJ, 636, L145

Le Bourlot, J., Pineau Des Forêts, G., Roueff, E., & Flower, D. R. 1993, A&A, 267, 233

Le Petit, F., Nehmé, C., Le Bourlot, J., & Roueff, E. 2006, ApJS, 64, 506

Maloney, P. R., Hollenbach, D. J., & Tielens, A. G. G. M. 1996, ApJ, 466, 561

Markwick, A. J., Ilgner, M., Millar, T. J., & Henning, Th. 2002, A&A, 385, 632

Mathis, J. S., Rumpl, W., & Nordsieck, K. H. 1977, ApJ, 217, 425

Najita, J. R., Carr, J. S., Glassgold, A. E., & Valenti, J. A. 2007, in Protostars and Planets V, ed. B. Reipurth, D. Jewitt, & K. Keil (Tucson: Univ. Arizona Press), 507

Opansky, B. J., & Leone, S. R. 1996, J. Phys. Chem., 100, 19904

Peeters, J., Van Look, H., & Ceursters, B. 1996, J. Phys. Chem., 100, 15124

Pety, J., Teyssier, D., Fossé, D., et al. 2005, A&A, 435, 885

Pitts, W. M., Pasternack, L., & McDonald, J. R. 1982, Chem. Phys., 68, 417

Semenov, D., Wiebe, D., & Henning, Th. 2004, A&A, 417, 93

Semenov, D., Wiebe, D., & Henning, Th. 2006, ApJ, 647, L60

Sterberg, A., & Dalgarno, A. 1995, ApJS, 99, 565

Teyssier, D., Fossé, D., Gerin, M., et al. 2004, A&A, 417, 135

Thi, W.-F., van Zadelhoff, G.-J., & van Dishoeck, E. F. 2004, A&A, 425, 955

van Dishoeck, E. F., Jonkheid, B., & van Hemert, M. C. 2006, Faraday Discuss., 133, 231

Willacy, K., & Langer, W. D. 2000, ApJ, 544, 903

Willacy, K., Klahr, H. H., Millar, T. J., & Henning, Th. 1998, A&A, 338, 995

Woodall, J., Agúndez, M., Markwick-Kemper, A. J., & Millar, T. J. 2007, A&A, 466, 1197

Woods, P. M., & Willacy, K. 2007, ApJ, 655, L49